Journal of Dermatological Science 93 (2019) 41–49

Contents lists available at ScienceDirect

Journal of Dermatological Science

journal homepage: www.jdsjournal.com

Original Article

Nanoparticle-mediated local delivery of pioglitazone attenuates bleomycin-induced skin fibrosis

Mai Kanemaru[a,b], Jun Asai[a,*], Jun-ichiro Jo[b], Takahiro Arita[a], Minako Kawai-Ohnishi[a], Miho Tsutsumi[a], Makoto Wada[a], Yasuhiko Tabata[b,**], Norito Katoh[a]

[a] Department of Dermatology, Kyoto Prefectural University of Medicine, Graduate School of Medical Science, Kyoto, Japan
[b] Laboratory of Biomaterials, Department of Regeneration Science and Engineering, Institute for Frontier Life and Medical Sciences, Kyoto University, Kyoto, Japan

ARTICLE INFO

Article history:
Received 17 July 2018
Received in revised form 24 October 2018
Accepted 27 November 2018

Keywords:
Poly(lactic-co-glycolic acid)
Controlled release
Nanoparticle
Peroxisome proliferator-activated receptor-γ
Pioglitazone
Fibrosis

ABSTRACT

Background: Nanoparticle-loaded delivery systems have attracted much attention recently. Poly(lactic-co-glycolic acid) (PLGA) is one of the most successful biodegradable polymers for biomedical applications. There are only a few studies on the treatment of dermal fibrosis with sustained-release drugs. Peroxisome proliferator-activated receptor-γ (PPAR-γ) plays an important role in endogenous anti-fibrotic defense mechanisms. Recent studies have suggested that pioglitazone, a synthetic PPAR-γ activator, has effects beyond reducing blood sugar and it can reduce fibrosis and inflammation when used systemically.

Objective: We aimed to assess the effects of local injections of pioglitazone-loaded PLGA nanoparticles (PGN-NP) on an experimental sclerosis and to demonstrate the *in vivo* pharmacokinetics of subcutaneously administered PLGA nanoparticles.

Methods: Locally injectable PGN-NP were prepared and subcutaneously administered to bleomycin (BLM)-induced scleroderma model mice. The effect of pioglitazone was also evaluated with cultured fibroblasts. Coumarin-6-loaded fluorescent PLGA nanoparticles (FL-NP) and silicon naphthalocyanine-loaded near-infrared PLGA nanoparticles (NIR-NP) were used to demonstrate *in vitro* cellular uptake by cultured fibroblasts and the *in vivo* pharmacokinetics of subcutaneously administered nanoparticles.

Results: Weekly subcutaneous injections of PGN-NP attenuated skin fibrosis in BLM-induced scleroderma model mice. Pioglitazone significantly suppressed migration ability and TGF-β-mediated myofibroblast differentiation in cultured fibroblasts. FL-NP were internalized into cultured fibroblasts within 60 min, and PGN-NP-primed fibroblasts expressed anti-fibrotic phenotypes. Subcutaneously injected NIR-NP remained in the vicinity of the injection site more than non-particulate silicon naphthalocyanine.

Conclusion: These results provide a basis for the development of new treatments for dermal fibrosis and a better understanding of the potential of PLGA nanoparticles in dermatology.

1. Introduction

Nano-sized drug carriers have attracted considerable attention recently. In the field of dermatology, various nanomaterials are used for topical drug delivery, dressings, and cosmetics [1,2]. Poly (lactic-co-glycolic acid) (PLGA) is one of the most successful biodegradable polymers to be developed. Among the different polymers developed to formulate polymeric nanoparticles, PLGA has attracted considerable attention due to its attractive properties, including its (i) biodegradability and biocompatibility, (ii)

Abbreviations: PLGA, poly(lactic-co-glycolic acid); PPAR-γ, peroxisome proliferator-activated receptor-γ; BLM, bleomycin; TGF-β, transforming growth factor-β; SSc, systemic sclerosis; α-SMA, α-smooth muscle actin; CTGF, connective tissue growth factor; HPLC, high-pressure liquid chromatography; DMSO, dimethyl sulfoxide; PGN-NP, pioglitazone-loaded poly(lactic-co-glycolic acid) nanoparticles; FL-NP, coumarin-6-loaded fluorescent poly(lactic-co-glycolic acid) nanoparticles; NIR-NP, silicon naphthalocyanine-loaded near-infrared fluorescent poly(lactic-co-glycolic acid) nanoparticles.

* Corresponding author at: Department of Dermatology, Kyoto Prefectural University of Medicine, Graduate School of Medical Science, 465, Kajii-cho, Kawaramachi-Hirokoji, Kamigyo-ku, Kyoto, 602-8566, Japan.
** Corresponding author at: Laboratory of Biomaterials, Department of Regeneration Science and Engineering, Institute for Frontier Life and Medical Sciences, Kyoto University, 53, Kawara-cho, Shogoin, Sakyo-ku, Kyoto, 606-8507, Japan.
E-mail addresses: jasai@koto.kpu-m.ac.jp (J. Asai), yasuhiko@infront.kyoto-u.ac.jp (Y. Tabata).

https://doi.org/10.1016/j.jdermsci.2018.11.012
0923-1811/

Food and Drug Administration (FDA) and European Medicine Agency approval as a drug delivery system for parenteral administration, (iii) well described formulations and methods of production adapted to various types of drugs, *e.g.* hydrophilic or hydrophobic small molecules or macromolecules, (iv) ability to protect against drug degradation, and (v) potential for sustained release [3]. PLGA has been used in sutures, drug delivery devices such as depot formulations of drugs, and tissue engineering scaffolds [4–6].

Scleroderma refers to a heterogeneous group of autoimmune fibrosing disorders, including localized scleroderma, limited cutaneous systemic sclerosis (SSc), and diffuse cutaneous SSc [7]. Vascular activation in SSc leads to the infiltration of inflammatory cells, endothelial to mesenchymal transition (EndoMT), and impaired coagulation/fibrinolysis [8]. Currently, there is no single drug used to treat SSc, with pharmacological approaches based on a combination of drugs that may be effective in treating organ damage or in relieving symptoms associated with visceral involvement [9]. Although there is no specific therapy for localized scleroderma either, a variety of therapeutic options, including topical corticosteroids and intralesional steroid therapy, are available [7].

An animal model of scleroderma has been established by repeated intradermal or subcutaneous injections of bleomycin (BLM) into the shaved back skins of mice [10,11]. In the model, cutaneous sclerosis is observed in the area surrounding the injection site [11]. Increasing evidence suggests that transforming growth factor-β (TGF-β) is a key mediator of tissue fibrosis in SSc as a consequence of extracellular matrix (ECM) accumulation. Many of the characteristics of SSc fibroblasts resemble those of normal fibroblasts stimulated by TGF-β, such as the elevated expression of collagen and α-smooth muscle actin (α-SMA). Moreover, connective tissue growth factor (CTGF) is induced by TGF-β and modulates fibroblast cell growth and ECM secretion [12].

Peroxisome proliferator-activated receptor-γ (PPAR-γ) is a nuclear orphan receptor and ligand-inducible transcription factor. Initially identified in adipocytes, PPAR-γ is widely expressed in mammalian tissues and regulates genes involved in not only lipid uptake, synthesis, and storage but also glucose metabolism; cell differentiation, survival, and proliferation; and immune and inflammatory responses. Prior studies have identified PPAR-γ as an important factor in endogenous anti-fibrotic defense mechanisms [13]. Pioglitazone (molecular weight, 356 Da) is a synthetic antidiabetic drug belonging to thiazolidinedione class that activates PPAR-γ. Like other PPAR-γ agonists, the anti-fibrotic and anti-inflammatory effects of pioglitazone have been reported [14,15].

The objective of this study was to establish a locally injectable, controlled-release matrix of pioglitazone for the treatment of skin fibrosis. PLGA was formed into nanoparticles containing pioglitazone, and these nanoparticles were used to establish an aqueous dispersion vehicle for the local delivery of pioglitazone. We hypothesized that the controlled release of pioglitazone from the subcutaneously administered nanoparticles would reduce skin fibrosis in BLM-induced scleroderma model mice. In addition, we sought to characterize the *in vitro* cellular uptake of fluorescent nanoparticles by cultured fibroblasts and the *in vivo* pharmacokinetics of subcutaneously administered near-infrared fluorescent nanoparticles.

2. Materials and methods

2.1. Preparation of nanoparticles and the in vitro *drug release profile*

Pioglitazone-loaded PLGA nanoparticles (PGN-NP), drug-free PLGA nanoparticles (Mock-NP, as a control), coumarin-6-loaded fluorescent PLGA nanoparticles (FL-NP), and silicon naphthalocyanine-loaded near-infrared fluorescent nanoparticles (NIR-NP) were prepared by an emulsion solvent evaporation method. The PGN-NP pioglitazone-release profile was determined *in vitro* in a tube containing phosphate-buffered saline (PBS) with 0.1% polysorbate-80 buffer at a constant rotation of 18 rpm and 37 °C.

2.2. BLM-induced scleroderma murine model

Balb/c mice were purchased from CLEA Japan, Inc. (Tokyo, Japan) and maintained under special pathogen-free conditions. Eight- to nine-week-old mice were used at the initial treatment. All animal protocols were approved by the Animal Care and Use Committee of Kyoto Prefectural University of Medicine.

Dermal fibrosis was induced by repeated subcutaneous injections of bleomycin sulfate (BLM; Adooq Bioscience, Irvine, CA, USA). BLM (100 μg/mouse, 0.5 mg/ml in PBS) was injected subcutaneously into the shaved dorsal skins of Balb/c mice with a 29-gauge needle (BLM mice). PBS instead of BLM was injected into the control mice. The injections were carried out four times per week for 3 weeks. During the 3 weeks of BLM injections, mice were treated in parallel by injection of PGN-NP (100 μg/mouse), Mock-NP (100 μg/mouse), or vehicle (PBS) once per week on days 1, 8, and 15. PGN-NP and Mock-NP were dispersed in PBS before injection. On day 22, mice were sacrificed and affected skin tissue was obtained. Blood glucose levels were measured with the Glucose PILOT Blood Glucose Monitoring System (Aventir Biotech, Carlsbad, CA, USA). Four to six animals were analyzed per experimental group.

2.3. In vitro *cell migration assay*

An *in vitro* cell migration assay was performed by scratching a cultured monolayer of human dermal fibroblasts (purchased from PromoCell GmbH, Heidelberg, Germany).

2.4. Myofibroblast differentiation

To induce myofibroblast differentiation, human dermal fibroblasts were stimulated with TGF-β1 (Thermo Fisher Scientific, Inc.) with or without pioglitazone treatment. For quantitative real-time reverse-transcription polymerase chain reaction (qRT-PCR) analysis, human dermal fibroblasts were grown to 75% confluence and transferred to reduced-serum medium (1% FBS). The cells were cultured in this medium for 15 h, followed by treatment with the indicated concentrations of pioglitazone or equal amounts of dimethyl sulfoxide (DMSO) for 30 min. Cells were then stimulated with TGF-β1 (10 ng/ml) for an additional 5 h. For western blotting analysis, human dermal fibroblasts in reduced-serum medium (1% FBS) were treated with the indicated concentrations of pioglitazone or equal amounts of DMSO for 15 h and stimulated with TGF-β1 (10 ng/ml) for an additional 24 h.

2.5. In vitro *cellular uptake of nanoparticles*

In vitro cellular uptake of nanoparticles by human dermal fibroblasts was visualized using FL-NP. Mock-NP were used as a negative control. Cells were incubated with 100 μg/ml of FL-NP or Mock-NP for up to 1 h and counter-stained with Hoechst 33258 (Polysciences, Inc., Warrington, PA, USA). The images were captured using a fluorescence microscope (BZ-X710, Keyence) with a 20× objective.

For qRT-PCR analysis, human dermal fibroblasts were treated with 100 μg/ml of PGN-NP or Mock-NP for 1 h, washed with PBS, and transferred to reduced-serum medium (1% FBS) free of

nanoparticles. Cells were cultured in the medium for 48 h, followed by stimulation with TGF-β1 (10 ng/ml) for an additional 5 h.

For immunocytochemistry, human dermal fibroblasts in reduced-serum medium (1% FBS) were treated with or without PGN-NP (100 μg/ml, without DMSO), Mock-NP (100 μg/ml) plus equivalent amounts of pioglitazone to that in PGN-NP (9.5 μM, with DMSO), or vehicle (DMSO) for 48 h, followed by stimulation with TGF-β1 (10 ng/ml) for an additional 48 h. Cells were then fixed in 4% paraformaldehyde. Three independent cultures were assessed for each condition.

2.6. In vivo *pharmacokinetics of subcutaneously administered nanoparticles*

The *in vivo* pharmacokinetics of the subcutaneously administered nanoparticles were assessed using NIR-NP with an IVIS Lumina III imaging system (PerkinElmer, Waltham, MA, USA). Balb/c mice were injected subcutaneously with NIR-NP (250 μg/mouse in 50 μl PBS). As a control, silicon 2,3-naphthalocyanine bis (trihexylsilyloxide) in acetone and PBS at a volume ratio of 1:9 or PBS alone was injected. The mice were imaged under anesthesia with an 845-nm emission filter after excitation with 780 nm for 20 s. Images were taken at several different time points after injection for up to 7 days. Organs (dorsal skin, ventral skin, inguinal lymph nodes, liver, spleen, heart, lung, and kidney) were collected 2 h and 7 days after injection and were also imaged after excitation for 10 s. Fluorescent signals were quantified using Living Image software (PerkinElmer). The total radiant efficiency (photons/s)/(μW/cm^2) of the mouse body image at each time point was measured, and the value at 0 h was set at 100%.

The materials and methods are explained in further detail in the Supplementary material.

3. Results

3.1. *Characterization and* in vitro *pioglitazone-release profile of nanoparticles*

The average diameters (± SD) of PGN-NP, FL-NP, NIR-NP, and Mock-NP were 305 ± 145 nm, 288 ± 143 nm, 283 ± 82 nm, and 285 ± 110 nm, respectively. All types of nanoparticles were negatively charged. HPLC study of FL-NP revealed a peak at 5.3 min, in the same location as the pure pioglitazone peak. The pioglitazone-loading content in the PGN-NP was 3.4 ± 0.07%. Fig. 1 shows the *in vitro* pioglitazone-release profile of PGN-NP. PGN-NP released 22.7 ± 3.5% of the incorporated pioglitazone within 24 h, and 52.0 ± 1.6% within 7 days, indicating sustained release of pioglitazone *in vitro*.

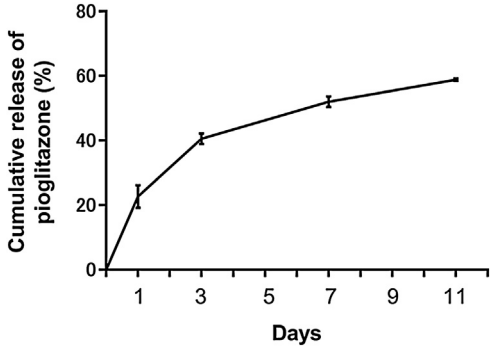

Fig. 1. *In vitro* pioglitazone-release profile of PGN-NP. Data are expressed as means ± SD (n = 4).

3.2. *Anti-fibrotic effects of PGN-NP on BLM-induced skin sclerosis*

Dermal thickness was examined in the images of HE-stained skin tissues collected from experimental mice (Fig. 2A and B). Collagen deposition was examined in the fluorescent images of Picrosirius red staining (Fig. 2C and D). Cells and elastic fibers were represented by green fluorescence under Picrosirius red staining. Both the dermal thickness and Picrosirius red-stained area increased in vehicle-treated BLM mice compared to those in vehicle-treated control mice ($P < 0.01$), indicating that BLM induced skin sclerosis in mice. The dermal thickness and Picrosirius red-stained area decreased in PGN-NP-treated BLM mice compared to those in vehicle- or Mock-NP-treated BLM mice ($P < 0.05$), indicating the anti-fibrotic effects of PGN-NP on BLM-induced skin sclerosis.

In the immunofluorescence staining images, the number of α-SMA-positive spindle-shaped cells was elevated in vehicle-treated BLM mice compared to that in vehicle-treated control mice ($P < 0.01$), indicating that BLM induced myofibroblast accumulation in the skin. The number of α-SMA-positive spindle-shaped cells was reduced in PGN-NP-treated BLM mice in comparison with numbers in Mock-NP-treated BLM mice ($P < 0.05$; Fig. 3A and B).

Fig. 3C and D show the relative expression levels of type I collagen (*Col1a1*) and TGF-β1 (*Tgfb1*) mRNA in the skin. *Col1a1* expression in vehicle-treated BLM mice increased compared to that in vehicle-treated control mice ($P < 0.05$), while *Col1a1* expression in PGN-NP-treated BLM mice decreased compared to that in vehicle-treated BLM mice ($P < 0.05$). Similarly, *Tgfb1* expression in PGN-NP-treated BLM mice tended to be lower than that in vehicle-treated BLM mice, but this difference was not significant.

We observed no obvious adverse events in Mock-NP- or PGN-NP-treated mice during the experiment, and there was no significant difference in blood glucose levels between PGN-NP-treated mice and the other groups at the end of the experiment (data not shown).

3.3. *Effects of pioglitazone on migration ability and myofibroblast differentiation in cultured human dermal fibroblasts*

Fig. 4A shows bright-field images taken at the beginning and end of an 8-h incubation period after the introduction of a scratch in the *in vitro* migration assay. The results showed that 50 μM pioglitazone treatment suppressed the migration ability of human dermal fibroblasts ($P < 0.01$; Fig. 4B). Fig. 4C shows the relative expression of *CTGF* mRNA in human dermal fibroblasts. TGF-β1 stimulation increased *CTGF* expression in DMSO-treated human dermal fibroblasts ($P < 0.01$), and this response was attenuated by pioglitazone treatment ($P < 0.05$ for 10 and 25 μM pioglitazone, $P < 0.01$ for 50 μM pioglitazone). Fig. 4D shows the results of the western blotting analysis of human dermal fibroblasts. TGF-β1 stimulation increased α-SMA protein expression in DMSO-treated human dermal fibroblasts, and this response was abrogated by 50 μM pioglitazone treatment. β-actin was used as an internal control.

3.4. In vitro *cellular uptake of nanoparticles by cultured human dermal fibroblasts*

The *in vitro* cellular uptake of FL-NP by human dermal fibroblasts was observed with fluorescent microscopy. As shown in Fig. 5A, cells incubated with 100 μg/ml FL-NP expressed green fluorescence in a granular form at 20 min after incubation. At 60 min after incubation, diffuse green fluorescence was observed in the cytoplasm.

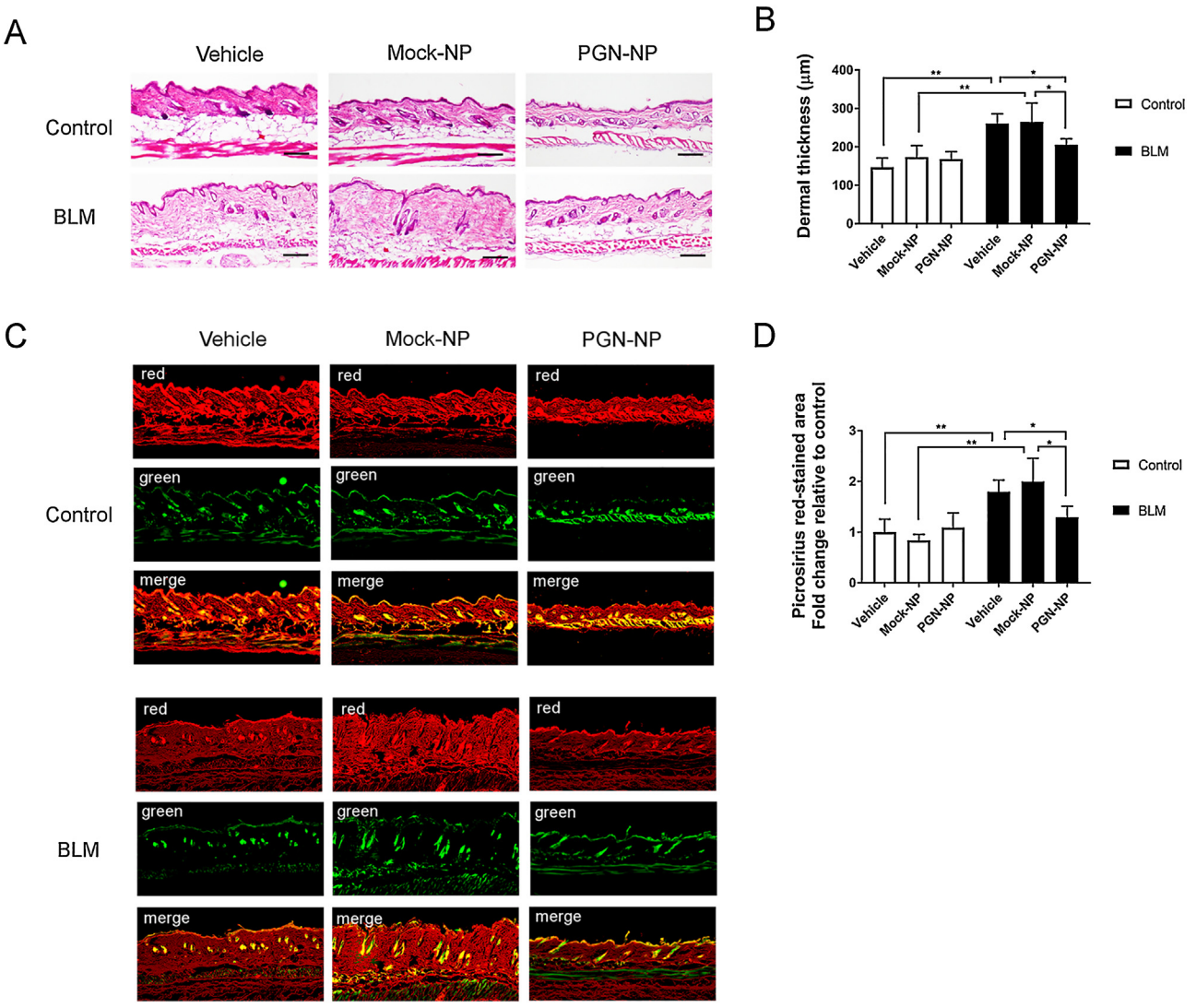

Fig. 2. Anti-fibrotic effects of PGN-NP on BLM-induced skin sclerosis. (A) HE-staining images of skin collected from mice. Bars = 300 μm. (B) Dermal thickness of BLM-induced scleroderma model mice. (C) Fluorescent images of Picrosirius red staining. Cells and elastic fibers are represented by green fluorescence. (D) Quantification of Picrosirius red-stained areas in BLM-induced scleroderma model mice. $^{*}P < 0.05$, $^{**}P < 0.01$ according to Tukey–Kramer multiple comparison test with n = 5–6 (B, D).

According to the results of qRT-PCR analysis, TGF-β1 stimulation increased *CTGF* expression in vehicle-treated human dermal fibroblasts ($P < 0.01$), and this response was attenuated by 1-h pretreatment with 100 μg/ml PGN-NP ($P < 0.01$). In addition, there was a significant difference in *CTGF* expression between Mock-NP-pretreated and PGN-NP-pretreated fibroblasts before TGF-β1 stimulation ($P < 0.05$; Fig. 5B). Similarly, α-SMA (*ACTA2*) expression tended to decrease in PGN-NP-pretreated fibroblasts compared to levels in vehicle- or Mock-NP-pretreated fibroblasts, but this difference was not significant (Fig. 5C). According to the immunocytochemical assay, α-SMA was present in the cytosol of TGF-β1-stimulated cells, and treatment with PGN-NP or Mock-NP plus equivalent amounts of pioglitazone to that contained in PGN-NP attenuated this response to the same extent (Fig. 5D). These data were confirmed in three experiments.

3.5. In vivo *pharmacokinetics of subcutaneously administered nanoparticles*

As shown in Fig. 6A, subcutaneously administered NIR-NP spread to the skin in the vicinity of the injection site. In contrast, non-particulate silicon naphthalocyanine fluoresced at the injection site only. Half ($50 \pm 10\%$) of the fluorescent signal was observed in the skin in NIR-NP-injected mice after 1 week, and this proportion was higher than that observed in the non-particulate silicon naphthalocyanine-injected mice (Fig. 6B, $P < 0.05$). Fig. 6C shows the *ex vivo* fluorescent images of the organs (dorsal skin, ventral skin, inguinal lymph nodes, liver, spleen, heart, lung, and kidney) collected at 2 h and 7 d after injection. Fluorescent signals were not detected in other organ other than the skin.

4. Discussion

Biomaterial-based drug delivery systems have been widely used to enhance local treatment effects and to reduce the frequency of administration. However, there are only a few studies on the treatment of dermal fibrosis with sustained-release drugs. For example, Ma et al. recently demonstrated that controlled delivery of a focal adhesion kinase inhibitor *via* pullulan collagen-based hydrogels accelerated the wound healing of excisional and burn wounds and reduced scar formation [16].

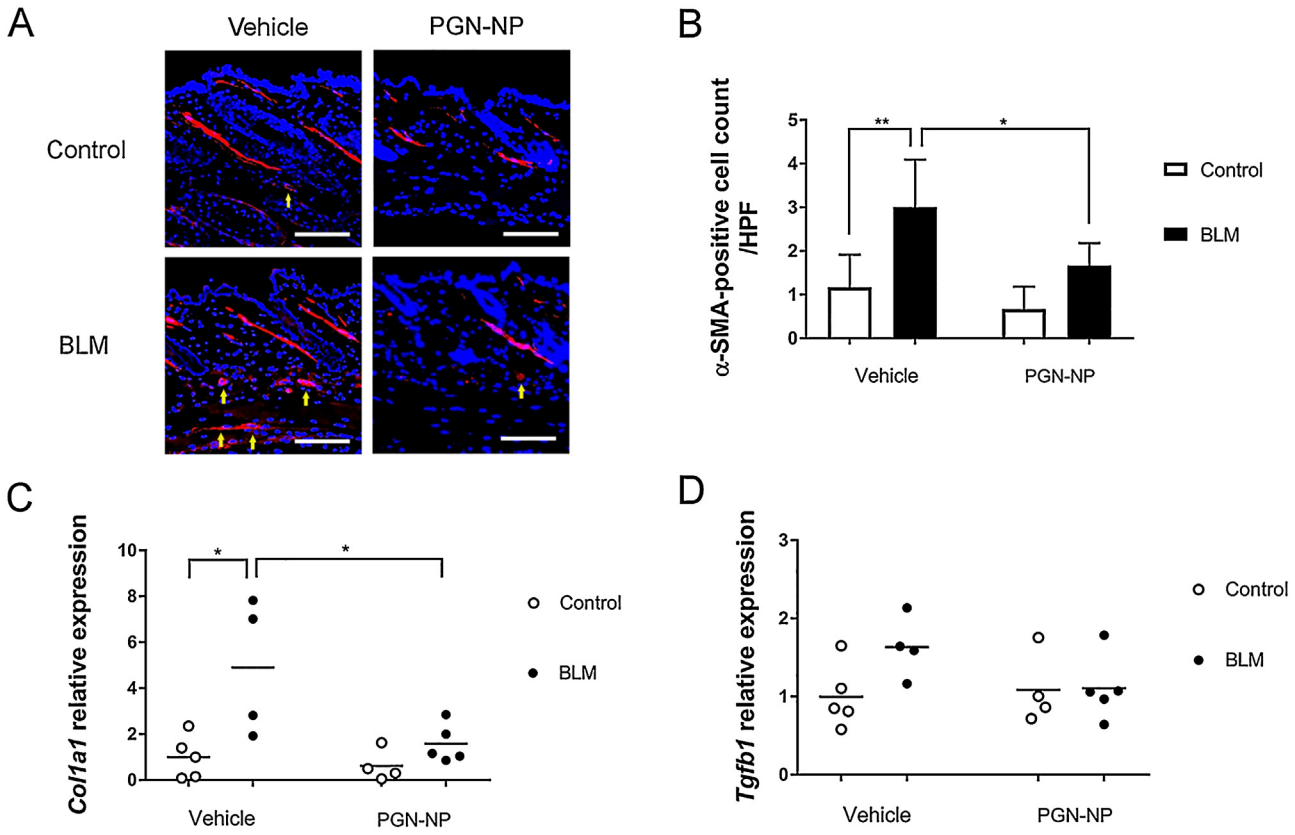

Fig. 3. Effects of PGN-NP on myofibroblast accumulation in BLM-induced skin sclerosis. (A, B) Immunofluorescence with antibodies against α-SMA (red fluorescence), counterstained with DAPI. α-SMA-positive spindle-shaped cells (yellow arrows) were counted. Bars = 100 μm. (C, D) Relative expression of *Col1a1* and *Tgfb1* mRNA in skin. Results were normalized to *Gapdh* expression, and the value in vehicle-treated control mice was set to 1.0. Data are expressed as means ± SD. $^{*}P < 0.05$, $^{**}P < 0.01$ according to Tukey–Kramer multiple comparison test with n = 5–6 (B) or n = 4–5 (C, D).

The activation of PPAR-γ by both natural and synthetic agonists can effectively inhibit pro-fibrotic tissue reactions, cell migration, and inflammation in many organs [17] and inhibit collagen synthesis in human keloid fibroblasts [18]. Systemic administration of the synthetic PPAR-γ agonist rosiglitazone has been shown to attenuate lung fibrosis in a BLM-induced pulmonary fibrosis model [19] and skin fibrosis in a BLM-induced scleroderma model [20]. In addition, rosiglitazone attenuates mononuclear cell activation [20]. PPAR-γ levels have been reported to be diminished in skin and lung tissues and in fibroblasts explanted from the lesional skin of SSc patients [13]. In normal fibroblasts, treatment with TGF-β downregulates PPAR-γ expression, and synthetic PPAR-γ agonists are capable of abrogating the pro-fibrotic responses of TGF-β, even in the presence of low PPAR-γ abundance [13]. However, systemic administration of thiazolidinediones is associated with fluid retention, which sometimes leads to congestive heart failure [21] and has a hypoglycemic effect. To avoid these systemic reactions, the topical use of pioglitazone with penetration enhancers has been investigated [22]; however, because of the hydrophobic property of pioglitazone, it is difficult to target the dermal layer through topical application and local injection.

Taking advantage of the anti-fibrotic effects of pioglitazone and the potential of PLGA as a sustained-release carrier of hydrophobic small molecules, we established locally injectable pioglitazone-loaded PLGA nanoparticles to treat an experimental dermal fibrosis. In this study, we confirmed the suppressive effects of pioglitazone on the migration ability and TGF-β-mediated myofibroblast differentiation of cultured fibroblasts, consistent with former reports on thiazolidinediones [14,20]. In BLM-induced scleroderma model mice, weekly subcutaneous injections of PGN-NP, but not Mock-NP, attenuated collagen deposition and myofibroblast accumulation without obvious adverse events relating to the application of nanoparticles or pioglitazone. Former studies have revealed the upregulation of TGF-β1 in the skins of BLM-induced scleroderma model mice [10] and the anti-inflammatory effects of thiazolidinediones [20]. In our study, changes in *Tgfb1* mRNA expression were not significant, but PGN-NP tended to decrease *Tgfb1* expression in the skins of BLM-induced scleroderma model mice.

Particle size is an important factor in the development of nanoparticles. We targeted the particle size 200–400 nm, hoping to enable both the cellular uptake of the particles and retention at the lesion site as a depot drug. Generally, cells internalize particles of 100–200 nm *via* receptor-mediated endocytosis and larger particles *via* phagocytosis [23]. Non-professional phagocytes may exhibit some phagocytic activity, but to a lower extent [24]. We visualized the cellular uptake of FL-NP by cultured human dermal fibroblasts using fluorescent imaging. In general, following the internalization of nanoparticles by pinocytosis, phagocytosis, or endocytosis, they were transported in vesicles from early endosomes to late endosomes and eventually to lysosomes. Alternatively, they escaped endo-lysosomes and diffused throughout the cytoplasm [3,25]. The release of drugs from the endosomes to the cytosol may occur due to osmotic swelling, direct membrane rupture, or other mechanisms [25]. In the present study, cells incubated with FL-NP

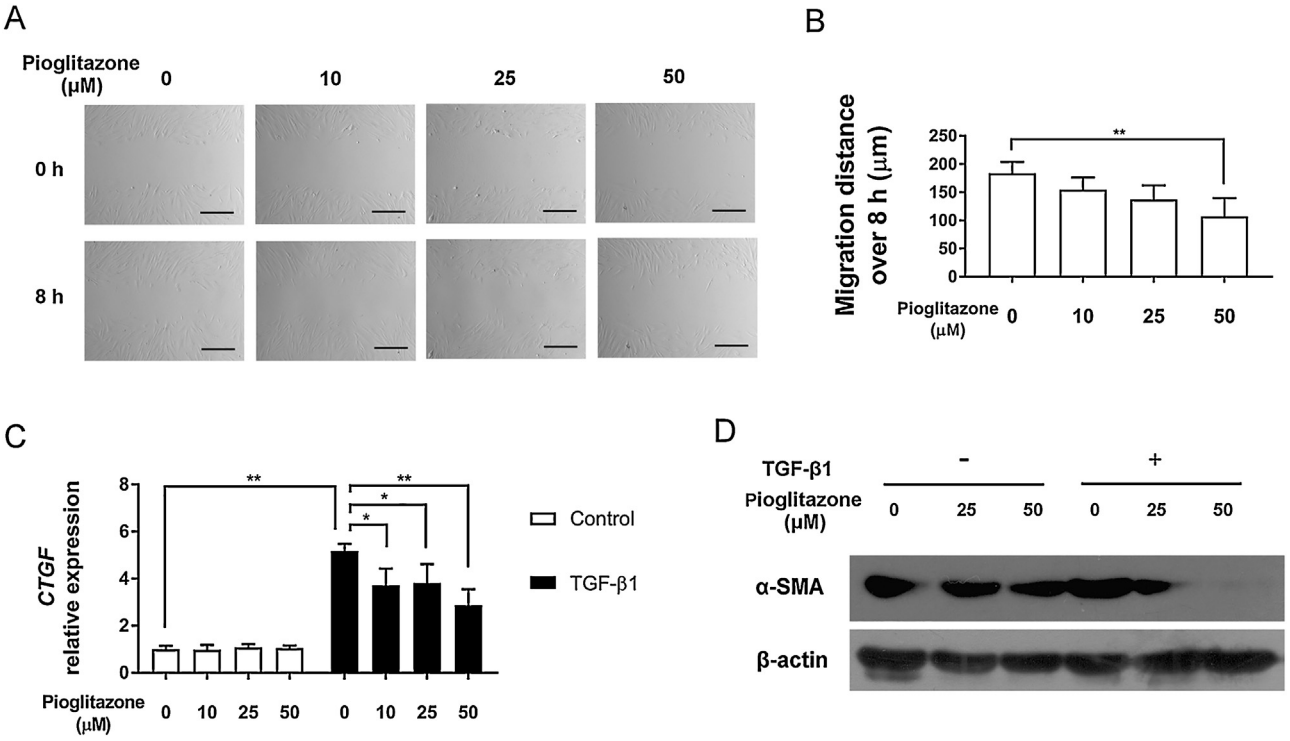

Fig. 4. Effects of pioglitazone on migration ability and myofibroblast differentiation in cultured human dermal fibroblasts. (A) Bright-field images of scratch assay at the beginning and end of an 8-h incubation period. Bars = 500 μm. (B) Quantification of migration ability of human dermal fibroblasts. (C) Relative expression of *CTGF* mRNA in human dermal fibroblasts. Results were normalized to *18S* rRNA expression, and the value in DMSO-treated control cells was set to 1.0. (D) Western blotting analysis of human dermal fibroblasts. β-actin was used as an internal control. Data are expressed as means ± SD. $^{*}P < 0.05$, $^{**}P < 0.01$ according to Dunnett's test *vs.* DMSO-treated control with n = 4 (B) or according to Tukey–Kramer multiple comparison test with n = 3 (C).

expressed green fluorescence in a granular form 20 min after incubation, and diffuse green fluorescence was observed in the cytoplasm 60 min after incubation. This phenomenon may be explained by the localization of the nanoparticles in endo-lysosomes (at 20 min), followed by the intracellular release of coumarin-6 into the cytosol (at 60 min). A similar phenomenon has been reported with smaller sized nanoparticles and occurred even more rapidly [26]. Fluorescent PLGA nanoparticles with a diameter of 69 ± 4 nm were observed in the endo-lysosomal compartments of cultured human arterial smooth muscle cells within 2 min of incubation and in the cytoplasmic compartments at >10 min post-incubation. The number of nanoparticles in the cytoplasm increased with increasing incubation time, indicating that following their uptake, the nanoparticles likely escaped rapidly from the endo-lysosomal compartments and entered the cytoplasm [26]. Furthermore, in the current study, 1-h incubation of the human dermal fibroblasts with PGN-NP attenuated the response of the fibroblasts to pro-fibrotic TGF-β1 stimulation *in vitro*, indicating the possibility of the intracellular degradation of nanoparticles and intracellular drug release. Cells treated for a longer duration with PGN-NP also expressed fewer fibrotic characters upon TGF-β1 stimulation, similarly to those treated with the equivalent amount of pioglitazone and Mock-NP. Considering that the amount of pioglitazone released from PGN-NP into the medium was less than 50%, cellular uptake of the nanoparticles may have increased the effect.

In addition to the cellular uptake, the distribution of nanoparticles in the body after administration also depends on the nanoparticle size [23]. In general, small drug molecules (<1 kDa) are thought to be preferentially absorbed by the blood capillaries after subcutaneous injection. In contrast, the absorption of small particles and macromolecules into the blood circulation is restricted. The lymphatics provide an alternative absorption pathway from the interstitial space for small particles (generally less than about 100 nm), but for larger colloidal materials (>100 nm), facile lymphatic access is lacking [27]. We evaluated the *in vivo* pharmacokinetics of NIR-NP by loading a hydrophobic near-infrared fluorescent material with a diameter of 283 ± 82 nm, imitating the size of PGN-NP. As a result, aqueous dispersion of the nanoparticles allowed them to spread to the skin in the vicinity of the injection site, and they remained in the area without accumulating in other organs.

It should be noted that there are some limitations of this study. First, we used normal human dermal fibroblasts in all *in vitro* experiments, rather than scleroderma fibroblasts. Second, due to the poor water solubility of pioglitazone, we were unable to compare the effect of PGN-NP injection in BLM-induced scleroderma model mice with that of free pioglitazone injection. However, one of the advantages to the incorporation of pioglitazone into nanoparticles is that it allows for dispersal in water.

Miller et al. demonstrated that tumor-associated macrophages serve as "drug depots" for the local delivery of nanotherapeutics to neighboring tumor cells [28]. Furthermore, since monocytes possess a unique ability to target and penetrate sites of inflammation, an approach to take advantage of the ability of monocytes to target and deliver polymeric particles to inflamed tissues has been reported [29]. Recently, more and more researchers have begun investigating new drug delivery systems utilizing cells such as antigen-specific T-cells, macrophages, and mesenchymal stem cells as cellular drug carriers [30]. Although in the present study we could not determine whether the target cells of PGN-NP were fibroblasts or included inflammatory cells as well, the communication between nanoparticles and the cells is of

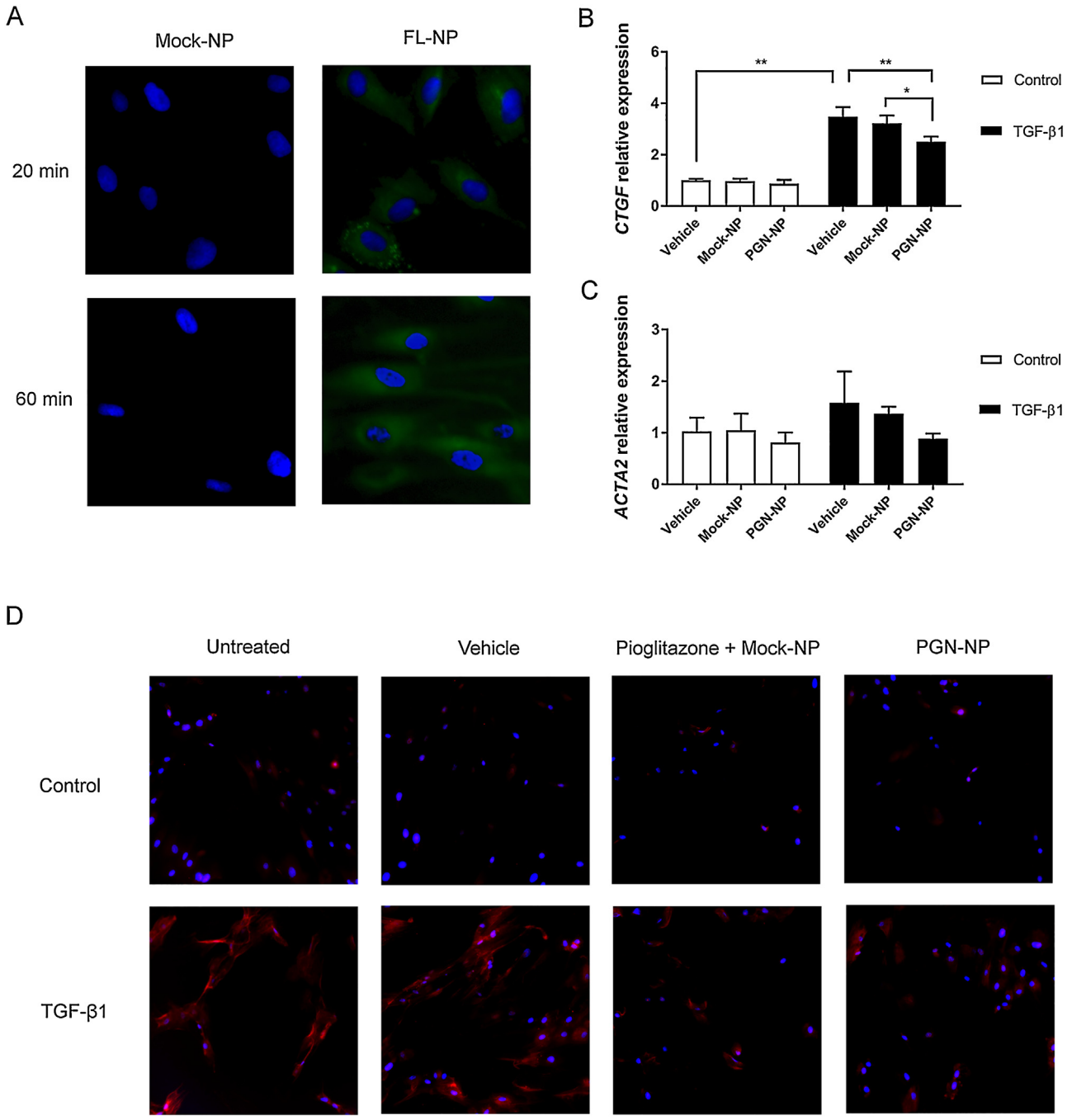

Fig. 5. *In vitro* cellular uptake of nanoparticles by cultured human dermal fibroblasts. (A) *In vitro* cellular uptake of FL-NP (green fluorescence) and Mock-NP by human dermal fibroblasts at 20 min and 60 min after incubation. Cells were counter-stained with Hoechst 33,258. (B, C) Relative expression of *CTGF* and *ACTA2* mRNA in human dermal fibroblasts. Results were normalized to *18S* rRNA expression, and the value in DMSO-treated controls was set to 1.0. Data are expressed as means ± SD. $^{*}P < 0.05$, $^{**}P < 0.01$ according to Tukey–Kramer multiple comparison test with n = 3. (D) Immunofluorescence with antibodies against α-SMA (red fluorescence), counterstained with DAPI. Human dermal fibroblasts were treated with or without PGN-NP, Mock-NP plus equivalent amounts of pioglitazone, or vehicle (DMSO) for 48 h, followed by stimulation with TGF-β1 (10 ng/ml) for an additional 48 h.

considerable interest. Further studies involving the *in vivo* imaging of fluorescent, luminescent, magnetic, or radioisotope nanoparticles are therefore required.

In conclusion, this study demonstrates that PLGA nanoparticle-mediated local delivery of pioglitazone attenuates skin fibrosis in BLM-induced scleroderma model mice by affecting the migration ability and TGF-β-mediated myofibroblast differentiation of fibroblasts. This drug delivery system is promising for the treatment of scleroderma, especially of the localized or limited types. Furthermore, thiazolidinediones are also promising for the treatment of other skin diseases, such as keloids [18] and scarring alopecia [15], and this technique of combining pioglitazone and PLGA might be useful in treating these as well. Since PLGA can be shaped into various forms, it can be applied either as a drug depot for systemic treatment or as a drug-eluting material for local treatment, such as in drug-eluting dressings, scaffolds, and sutures. Further applications in clinical settings are therefore expected.

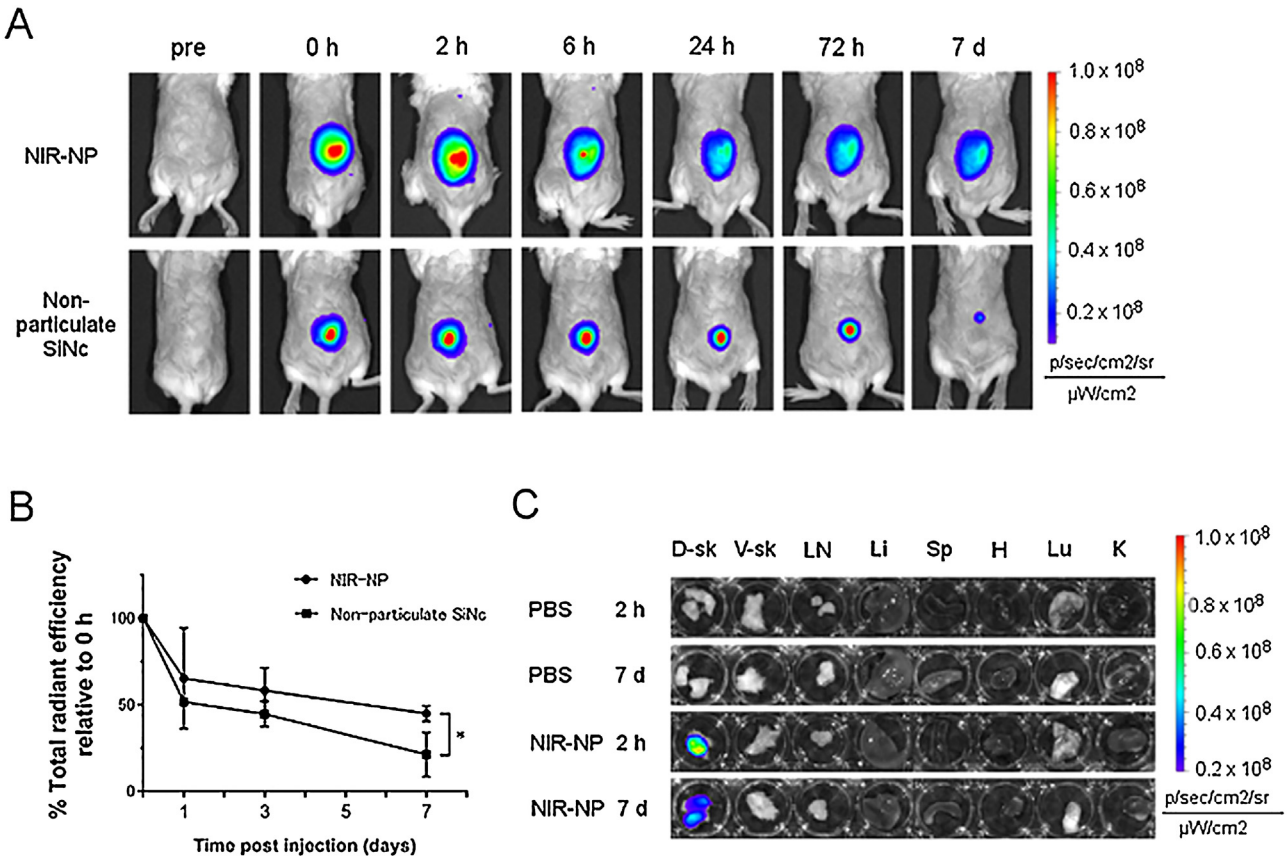

Fig. 6. *In vivo* pharmacokinetics of nanoparticles. (A) *In vivo* images of NIR-NP and non-particulate silicon naphthalocyanine (SiNc) at several different time points after subcutaneous injection into the dorsal skin. (B) Quantification of fluorescence signal relative to that obtained at 0 h. Data are expressed as means ± SD. $^*P < 0.05$ according to Student's *t*-test with n = 3. (C) Fluorescence distribution in the organs at 2 h and 7 days after the subcutaneous injection of NIR-NP into the dorsal skin. D-sk, dorsal skin; V-sk, ventral skin; LN, lymph nodes; Li, liver; Sp, spleen; H, heart; Lu, lung; K, kidney.

Funding

This work was supported by SENSHIN Medical Research Foundation (grant number: MTPS20160425013). The sponsor had no control over the research design, analysis, interpretation, writing, or publication.

Conflict of interest

The authors state no conflict of interest.

Acknowledgements

The authors wish to thank the current and former members of the Laboratory of Biomaterials at Kyoto University for useful advice on the preparation and characterization of the nanoparticles. The authors also thank S. Kotani at Kyoto Prefectural University of Medicine for technical advice.

Appendix A. Supplementary data

Supplementary material related to this article can be found, in the online version, at doi:https://doi.org/10.1016/j.jdermsci.2018.11.012.

References

[1] J.R. Antonio, C.R. Antônio, I.L.S. Cardeal, J.M.A. Ballavenuto, J.R. Oliveira, Nanotechnology in dermatology, An. Bras. Derm. Sifilogr. 89 (2014) 126–136.
[2] Z. Zhang, P.-C. Tsai, T. Ramezanli, B.B. Michniak-Kohn, Polymeric nanoparticles-based topical delivery systems for the treatment of dermatological diseases, Wiley Interdiscip. Rev. Nanomed. Nanobiotechnol. 5 (2013) 205–218.
[3] F. Danhier, E. Ansorena, J.M. Silva, R. Coco, A. Le Breton, V. Préat, PLGA-based nanoparticles: an overview of biomedical applications, J. Control. Release 161 (2012) 505–522.
[4] K.A. Athanasiou, G.G. Niederauer, C.M. Agrawal, Sterilization, toxicity, biocompatibility and clinical applications of polylactic acid/polyglycolic acid copolymers, Biomaterials 17 (1996) 93–102.
[5] D.S. Annis, D.F. Mosher, D.D. Roberts, Injectable controlled release depots for large molecules, J. Control. Release 28 (2014) 240–253.
[6] B.D. Ulery, L.S. Nair, C.T. Laurencin, Biomedical applications of biodegradable polymers, J. Polym. Sci. Part B: Polym. Phys. 49 (2011) 832–864.
[7] C. Ferreli, G. Gasparini, A. Parodi, E. Cozzani, F. Rongioletti, L. Atzori, Cutaneous manifestations of scleroderma and scleroderma-like disorders: a comprehensive review, Clin. Rev. Allergy Immunol. 53 (2017) 306–336.
[8] Y. Asano, Systemic sclerosis, J. Dermatol. 45 (2018) 128–138.
[9] M. Cossu, L. Beretta, P. Mosterman, M.J.H. de Hair, T.R.D.J. Radstake, Unmet needs in systemic sclerosis understanding and treatment: the knowledge gaps from a scientist's, clinician's, and patient's perspective, Clin. Rev. Allergy Immunol. (2017), doi:http://dx.doi.org/10.1007/s12016-017-8636-1 Epub ahead of print.
[10] T. Yamamoto, S. Takagawa, I. Katayama, K. Yamazaki, Y. Hamazaki, H. Shinkai, K. Nishioka, Animal model of sclerotic skin. I: local injections of bleomycin induce sclerotic skin mimicking scleroderma, J. Invest. Dermatol. 112 (1999) 456–462.
[11] T. Yamamoto, Animal model of systemic sclerosis, J. Dermatol. 37 (2010) 26–41.
[12] H. Ihn, Autocrine TGF-β signaling in the pathogenesis of systemic sclerosis, J. Dermatol. Sci. 49 (2008) 103–113.
[13] J. Wei, A.K. Ghosh, J.L. Sargent, K. Komura, M. Wu, Q.Q. Huang, M. Jain, M.L. Whitfield, C. Feghali-Bostwick, J. Varga, PPARγ downregulation by TGF in fibroblast and impaired expression and function in systemic sclerosis: a novel mechanism for progressive fibrogenesis, PLoS One 5 (2010) e13778.
[14] Y. Aoki, T. Maeno, K. Aoyagi, M. Ueno, F. Aoki, N. Aoki, J. Nakagawa, Y. Sando, Y. Shimizu, T. Suga, M. Arai, M. Kurabayashi, Pioglitazone, a peroxisome

proliferator-activated receptor gamma ligand, suppresses bleomycin-induced acute lung injury and fibrosis, Respiration 77 (2009) 311–319.
[15] M.J. Harries, R. Paus, Scarring alopecia and the PPAR-γ connection, J. Invest. Dermatol. 129 (2009) 1066–1070.
[16] K. Ma, S.H. Kwon, J. Padmanabhan, D. Duscher, A.A. Trotsyuk, Y. Dong, M. Inayathullah, J. Rajadas, G.C. Gurtner, Controlled delivery of a focal adhesion kinase inhibitor results in accelerated wound closure with decreased scar formation, J. Invest. Dermatol. (2018), doi:http://dx.doi.org/10.1016/j.jid.2018.04.034 Epub ahead of print.
[17] A.A. Kulkarni, T.H. Thatcher, K.C. Olsen, S.B. Maggirwar, R.P. Phipps, P.J. Sime, PPAR-γ ligands repress TGFβ-induced myofibroblast differentiation by targeting the PI3K/Akt pathway: implications for therapy of fibrosis, PLoS One 6 (2011) e15909.
[18] H.Y. Zhu, W.D. Bai, H.T. Wang, S.T. Xie, K. Tao, L.L. Su, J.Q. Liu, X.K. Yang, J. Li, Y.C. Wang, T. He, J.T. Han, D.H. Hu, Peroxisome proliferator-activated receptor-γ agonist inhibits collagen synthesis in human keloid fibroblasts by suppression of early growth response-1 expression through upregulation of miR-543 expression, Am. J. Cancer Res. 6 (2016) 1358–1370.
[19] T. Genovese, S. Cuzzocrea, R. Di Paola, E. Mazzon, C. Mastruzzo, P. Catalano, M. Sortino, N. Crimi, A.P. Caputi, C. Thiemermann, C. Vancheri, Effect of rosiglitazone and 15-deoxy-Δ12,14-prostaglandin J2 on bleomycin-induced lung injury, Eur. Respir. J. 25 (2005) 225–234.
[20] M. Wu, D.S. Melichian, E. Chang, M. Warner-Blankenship, A.K. Ghosh, J. Varga, Rosiglitazone abrogates bleomycin-induced scleroderma and blocks profibrotic responses through peroxisome proliferator-activated receptor-β, Am. J. Pathol. 174 (2009) 519–533.
[21] R.M. Lago, P.P. Singh, R.W. Nesto, Congestive heart failure and cardiovascular death in patients with prediabetes and type 2 diabetes given thiazolidinediones: a meta-analysis of randomised clinical trials, Lancet 370 (2007) 1129–1136.
[22] M. Silva-Abreu, L.C. Espinoza, M.J. Rodríguez-Lagunas, M.-J. Fábrega, M. Espina, M.L. García, A.C. Calpena, Human skin permeation studies with PPARγ agonist to improve its permeability and efficacy in inflammatory processes, Int. J. Mol. Sci. 18 (2017) 2548–2565.
[23] W. Huang, C. Zhang, Tuning the size of poly(lactic-co-glycolic acid) (PLGA) nanoparticles fabricated by nanoprecipitation, Biotechnol. J. 13 (2018) 1700203.
[24] H. Hillaireau, P. Couvreur, Nanocarriers' entry into the cell: relevance to drug delivery, Cell. Mol. Life Sci. 66 (2009) 2873–2896.
[25] S. Barua, S. Mitragotri, Challenges associated with penetration of nanoparticles across cell and tissue barriers: a review of current status and future prospects, Nano Today 9 (2014) 223–243.
[26] J. Panyam, W.Z. Zhou, S. Prabha, S.K. Sahoo, V. Labhasetwar, Rapid endo-lysosomal escape of poly(DL-lactide-co-glycolide) nanoparticles: implications for drug and gene delivery, FASEB J. 16 (2002) 1217–1226.
[27] D.N. McLennan, C.J.H. Porter, S.A. Charman, Subcutaneous drug delivery and the role of the lymphatics, Drug Discov. Today Technol. 2 (2005) 89–96.
[28] M.A. Miller, Y.R. Zheng, S. Gadde, C. Pfirschke, H. Zope, C. Engblom, R.H. Kohler, Y. Iwamoto, K.S. Yang, B. Askevold, N. Kolishetti, M. Pittet, S.J. Lippard, O.C. Farokhzad, R. Weissleder, Tumour-associated macrophages act as a slow-release reservoir of nano-therapeutic Pt(IV) pro-drug, Nat. Commun. 6 (2015) 8692.
[29] A.C. Anselmo, J.B. Gilbert, S. Kumar, V. Gupta, R.E. Cohen, M.F. Rubner, S. Mitragotri, Monocyte-mediated delivery of polymeric backpacks to inflamed tissues: a generalized strategy to deliver drugs to treat inflammation, J. Control. Release 199 (2015) 29–36.
[30] P. Tiet, J.M. Berlin, Exploiting homing abilities of cell carriers: targeted delivery of nanoparticles for cancer therapy, Biochem. Pharmacol. 145 (2017) 18–26.